Nanotechnology

Hydrogen-Bonded CdS Nanoparticle Assemblies on Electrodes for Photoelectrochemical Applications**

Ronan Baron, Chih-Hao Huang, Dario M. Bassani, Avital Onopriyenko, Maya Zayats, and Itamar Willner**

The organization of functional semiconductor nanoparticles on surfaces has been extensively examined in recent years,[1] and the use of organized semiconductor nanoparticle systems for photoelectrochemical applications has attracted specific research efforts.[2] For example, core–shell nanoparticle systems were reported to behave as organized matrices that assist charge separation and enhance photocurrent generation when deposited on electrodes.[3] Similarly, the electropolymerization of CdS semiconductor nanoparticles in conductive bis-aniline films proved to result in an organized system that facilitated the charge separation of electron–hole pairs, generated upon photoexcitation of the semiconductor nanoparticles, and the transport of conduction-band electrons to the electrode and led to improved photocurrents.[4] The deposition of layered semiconductor nanoparticles on surfaces by using electrostatic interactions[5] or covalent bonds[6] has been described. Likewise, the assembly of semiconductor nanoparticles on electrode supports by using molecular[7] or supramolecular[8] cross-linkers and hybrid layered metal nanoparticle/semiconductor nanoparticle assemblies[9a] or carbon nanotube/semiconductor nanoparticle systems[9b] were studied. The relationship between structure and photoelectrochemical function in these nanostructures was characterized, and the assembly of these hybrid systems proved to be an effective means to improve the generation of photocurrents by assisting charge separation.

In other organized systems, hydrogen-bonded interactions are an important motif in the generation of supramolecular structures.[10] However, the use of hydrogen bonds to assemble nanoparticle structures has been less explored. The aggregation of silver nanoparticles[11] or gold nanoparticles[12] by interparticle hydrogen bonds of the capping monolayers was reported. Also, modified gold nanoparticles that form hydrogen-bonded host–guest complexes have been synthesized[13] and applied to the development of an electrochemical sensor for phosphate.[13b] To date, the use of hydrogen bonds to fabricate layered nanoparticle structures on surfaces is little explored, but the formation of a multilayer of gold nanoparticles, modified by carboxylic acids, using polyvinylpyridine as the cross-linker in a layer-by-layer deposition process was examined.[14] However, the assembly of functional hydrogen-bonded layered nanoparticle structures on surfaces is unknown. Herein, we report the assembly of cadmium sulfide nanoparticles and gold nanoparticle/cadmium sulfide nanoparticle hybrids on gold surfaces through complementary barbiturate–triaminodiazine hydrogen-bonded interactions and the application of the systems for the generation of photocurrents.

The thioacetyl-protected barbiturate **1** and its complementary hydrogen-bonding aminopyrimidine partner **3** (Scheme 1) were used to modify the CdS or Au nanoparticles.

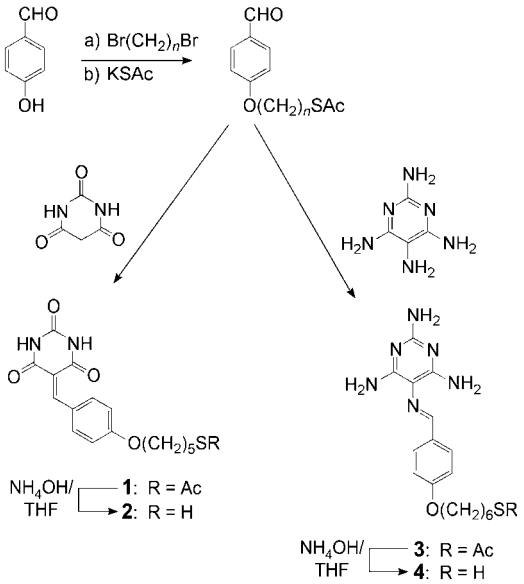

Scheme 1. Synthesis and structures of barbiturate compounds **1** and **2** as well as their triaminodiazine complements **3** and **4**. $n = 5$ for **1** and **2**; $n = 6$ for **3** and **4**.

The capped nanoparticles were then organized on surfaces by using complementary hydrogen bonds as the driving force. The CdS nanoparticles (4–5 nm diameter) were prepared according to reported methods,[15] and the resulting nanoparticles were treated in a solution of heptane/THF with the thiol derivatives **2** or **4**. The average loading of the CdS nanoparticles with **2** or **4** was determined spectroscopically by monitoring the absorption spectra of the CdS nanoparticles in solution before and after thiol modification. The subtraction of the respective absorbance spectra led to the net absorbance of the capping reagents associated with the CdS nanoparticles.

[*] C.-H. Huang, Dr. D. M. Bassani
Centre de Recherche en Chimie Moléculaire
LCOO CNRS UMR 5802
Université Bordeaux 1
351, Cours de la Libération, 33405 Talence cedex (France)
Fax: (+33) 5-4000-6158
E-mail: d.bassani@lcoo.u-bordeaux1.fr
Dr. R. Baron, A. Onopriyenko, M. Zayats, Prof. I. Willner
Institute of Chemistry and
the Farkas Center for Light-Induced Processes
The Hebrew University of Jerusalem
Jerusalem 91904 (Israel)
Fax: (+972)-2-652-7715
E-mail: willnea@vms.huji.ac.il

[**] This work was supported by the German–Israeli Program (DIP) as well as the French MRT and CNRS (AC Nanosciences–Nanotechnologies). M.Z. acknowledges the Israeli Ministry of Science for a Levi Eshkol fellowship. The authors are grateful to Prof. D. Mandler and A. Becker (The Hebrew University of Jerusalem) for assistance with the FTIR measurements.

Supporting information for this article is available on the WWW under http://www.angewandte.org or from the author.

  DOI: 10.1002/ange.200463055

From the absorbance value at $\lambda = 270$ nm of a solution of known concentration of the CdS nanoparticles (the extinction coefficient (ε) of 4–5-nm CdS nanoparticles is $7 \times 10^5\,\text{M}^{-1}\,\text{cm}^{-1}$),[16] we estimate the average loading of **2** and **4** to be 172 and 190 units per particle, respectively.

Figure 1 depicts the methods to assemble the hydrogen-bonded CdS nanoparticles on gold electrodes. The systems were assembled on Au/quartz piezoelectric crystals to enable

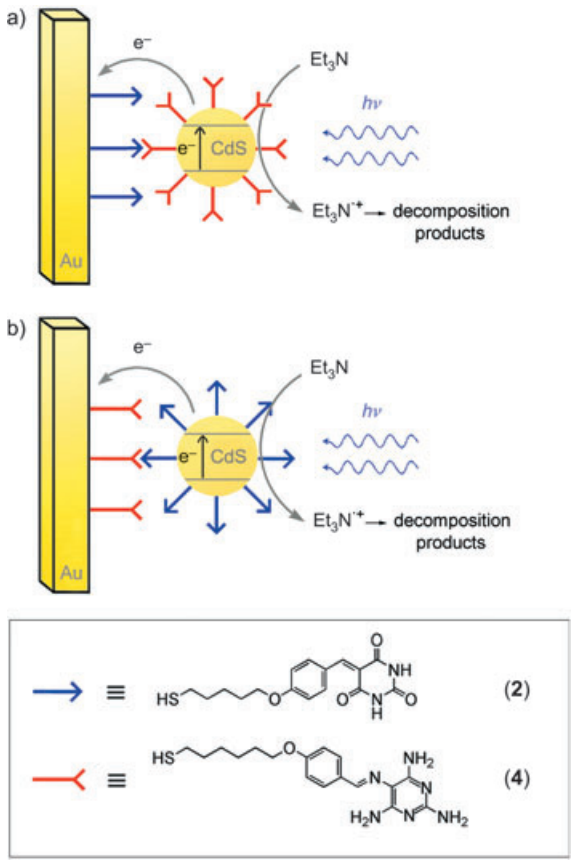

Figure 1. Schematic presentation of hydrogen-bonded CdS nanoparticle assemblies in which a) **2** is bound to the gold electrode and **4** is bound to the CdS nanoparticles, and b) **4** is bound to the electrode and **2** is associated with the CdS nanoparticles.

the characterization of the loading of the different components on the surfaces by microgravimetric quartz-crystal-microbalance (QCM) analyses. In one configuration, Figure 1 a, the thiolated barbiturate **2** was linked to the Au/quartz surface. From the frequency change (Δf), its surface coverage was calculated to be 6.6×10^{-10} mole cm^{-2}. The monolayer-modified surface was then treated with the **4**-functionalized CdS nanoparticles in dry THF. From the frequency change ($\Delta f = -420$ Hz in air), we estimate the surface coverage of the CdS nanoparticles to be 3.1×10^{12} particles cm^{-2} (note, the calculation took into account the loading of the CdS nanoparticles with **4**). Thus, presumably, about 32 monolayer units participate in the hydrogen-bonded association of a CdS nanoparticle to the surface. Further support that the CdS nanoparticles are linked to the electrode by hydrogen bonds was obtained by FT-IR experiments. For the monolayer of thiolated barbiturate **2** on the gold-coated glass, a broad band at $\tilde{\nu} = 3250$ cm^{-1} for the N-H group and three sharp bands at $\tilde{\nu} = 1747$, 1716, and 1687 cm^{-1} for the three different carbonyl functionalities were observed. These bands are consistent with the reported values of IR peaks for barbiturate derivatives.[17] A drop of a solution that contained the CdS nanoparticles capped with the thiolated triaminodiazine **4** was dried on the gold surface, and the residue revealed a broad band at $\tilde{\nu} = 3255$ cm^{-1} (N-H) and an intense band at 1574 cm^{-1} (C=N). For the hydrogen-bonded assembly in which the **4**-capped CdS nanoparticles are linked to the **2**-functionalized gold surface, two bands at $\tilde{\nu} = 3262$ and 3031 cm^{-1} were observed. The appearance of a wide band at $\tilde{\nu} = 3031$ cm^{-1} was previously attributed to the hydrogen-bonded N–H bond between the aminoazine and barbiturate carbonyl functionalities.[18] Similarly, the three sharp bands of the carbonyl group of the barbiturate monolayer are reduced to two bands and shifted to $\tilde{\nu} = 1702$ and 1698 cm^{-1} upon formation of the hydrogen-bonded assembly with the **4**-capped CdS nanoparticles. These shifts are in good agreement with the reported IR bands of hydrogen-bonded assemblies between barbiturate and triaminodiazine derivatives.[17]

In the second configuration of the hydrogen-bonded CdS nanoparticles, as depicted in Figure 1 b, **4** was assembled on the Au/quartz crystal with a surface coverage of 6.4×10^{-10} mole cm^{-2}. The **2**-functionalized CdS nanoparticles were then bound through hydrogen bonds to the surface with a surface coverage of 3.3×10^{12} particles cm^{-2}. The formation of this hydrogen-bonded CdS nanoparticle assembly was also supported by FTIR measurements. Similar to the spectral changes discussed in detail above for system a, analogous shifts for system b were observed. New stretching frequencies for the hydrogen-bonded carbonyl group at $\tilde{\nu} =$ 1700 and 1705 cm^{-1} as well as the non-bonded carbonyl functionalities associated with the particles at $\tilde{\nu} = 1730$, 1716, and 1683 cm^{-1} are the most indicative bands for the formation of the hydrogen-bonded system. A new, less intense band at $\tilde{\nu} = 3035$ cm^{-1}, which corresponds to the hydrogen-bonded N–H bond to the barbiturate carbonyl functions that cap the CdS nanoparticles, was also observed.

The resulting surfaces were also characterized by absorption spectroscopy. Figure 2 a shows the absorption spectrum of the gold surface functionalized with CdS nanoparticles, generated by the association of the **4**-modified CdS nanoparticles with the **2**-functionalized surface. Figure 2 b shows the photocurrent action spectrum of the electrodes modified with CdS nanoparticles, prepared according to system a (Figure 1 a). The photocurrents were recorded in anhydrous THF in the presence of triethylamine (Et_3N) as the electron donor and tetra-*n*-butylammonium hexafluorophosphate as the electrolyte. The photocurrent action spectrum follows the absorbance pattern of the CdS nanoparticles. Furthermore, control experiments indicated that in the absence of either the electron donor or the CdS nanoparticles, no photocurrent was generated in the system. Figure 2 c shows the effect of the applied potential on the magnitude of the resulting photocurrent. As the applied potential is negatively shifted, the photocurrent decreases and is completely blocked at about −0.5 V (vs SCE). These results allow us to define the

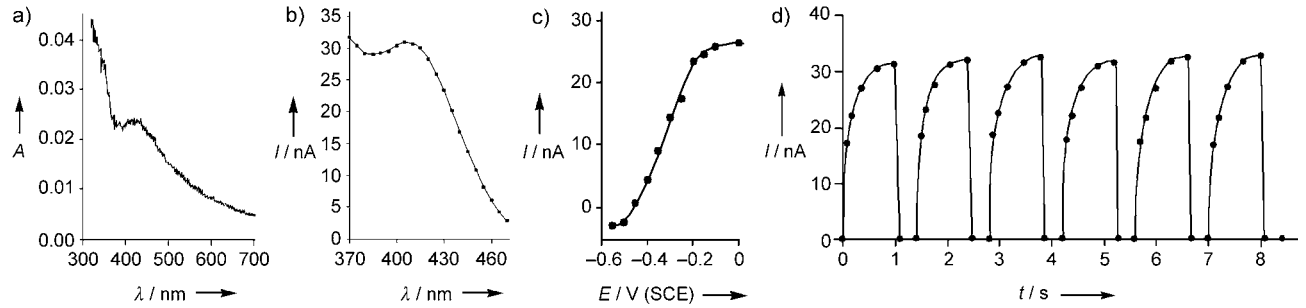

Figure 2. a) Absorbance spectrum of the CdS nanoparticle layer on a gold-coated glass support prepared according to Figure 1 a; b) photocurrent action spectrum corresponding to the CdS nanoparticle assembly shown in Figure 1 a; c) photocurrent recorded as a function of the applied potential at $\lambda = 410$ nm (SCE = standard calomel electrode); d) light-induced "ON" and "OFF" states of switchable photocurrents generated upon irradiation of the functionalized electrode at $\lambda = 410$ nm. All data were recorded in THF solutions containing triethylamine (2×10^{-2} M) and tetra-*n*-butylammonium hexafluorophosphate (0.1 M).

mechanism for the generation of photocurrents in the system. Upon photoexcitation of the CdS nanoparticles, an electron–hole pair is generated in the nanoparticles. The transfer of conduction-band electrons to the electrode followed by the oxidation of the electron donor by valence-band holes leads to the formation of the steady-state photocurrent. Biasing the electrode potential at −0.5 V (vs SCE) blocks the transfer of conduction-band electrons to the electrode which prohibits the generation of photocurrents. By knowing the absorbance features of the CdS nanoparticle interface, the efficiency of light to electrical-energy conversion was calculated to be 0.5%. The functionalized electrode revealed reasonable stability. Figure 2 d shows the cyclic "ON" and "OFF" formation of light-induced photocurrents in the system. The electrode was stable for at least 3 days upon storage in the dark under dry conditions, whilst less than 10% decrease in the photocurrents were observed after immersion for 5 hours in the THF/electrolyte solution.

Further support that the CdS nanoparticle interface is stabilized by hydrogen-bonding interactions was obtained by examining the effect on the resulting photocurrent of the addition of 10% water to the THF/electrolyte solution (Figure 3). As the time interval after the addition of H_2O becomes longer, the resulting photocurrent decreases. Simultaneous QCM analyses indicated that the addition of H_2O to the CdS nanoparticle modified Au/quartz surface resulted in the dissociation of CdS nanoparticles from the electrode support. Interestingly, however, we did not notice desorbtion of the photoactive interface within 10 minutes after the addition of 2% H_2O to the THF/electrolyte solution. Increasing the concentration of H_2O enhanced the dissociation rate of the CdS nanoparticles. The relative stability of the CdS nanoparticle interface is therefore attributed to the multipoint hydrogen-bonded association of the nanoparticles to the monolayer which results in the synergetic binding of the nanoparticles to the surface.

The photocurrent action spectrum observed for the system described in Figure 1 b is depicted in the Supporting Information. The efficiency of conversion of light to electrical energy in this system was estimated to be about 0.4%. This electrode reveals similar properties and functions to the electrode configuration outlined in Figure 1 a. The addition of

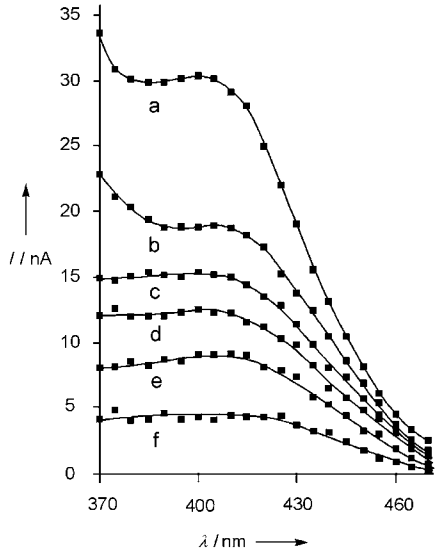

Figure 3. Effect of added water on the photocurrent spectra generated by the CdS nanoparticle assembly shown in Figure 1 a. Data recorded in THF solutions containing triethylamine (2×10^{-2} M) and tetra-*n*-butylammonium hexafluorophosphate (0.1 M). Photocurrent spectra were recorded a) before and (b–f) after the addition of 10% water to the solution in THF: b) 4 min, c) 8 min, d) 12 min, e) 16 min, and f) 20 min.

10% of H_2O to this system similarly resulted in the time-dependent degradation of the hydrogen-bonded interface and decrease of the photocurrent.

In light of previous observations that employed layered gold nanoparticle/CdS nanoparticle hybrid systems for the enhanced generation of photocurrents,[9a] we decided to use hydrogen bonds as a means to construct gold nanoparticle/CdS nanoparticle composites (Figure 4). Citrate-stabilized gold nanoparticles[19] (12 ± 1 nm) were linked by a thiolated monolayer to a Au/quartz surface and a semitransparent (Au film thickness ≈ 50 nm) gold-coated glass slide. Then a monolayer of **4** was assembled on the gold nanoparticles, with an average loading of 5.8×10^3 molecules of **4** per particle determined by QCM measurements. CdS nanoparticles functionalized with **2** were then linked through hydrogen bonds to the gold nanoparticles. QCM measurements of the

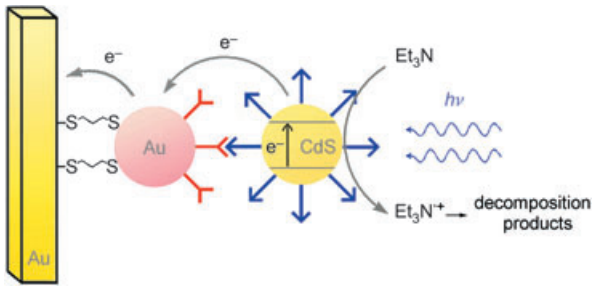

Figure 4. Schematic representation of the layered hydrogen-bonded gold nanoparticle/CdS nanoparticle assembly associated with a gold electrode in which the gold nanoparticles are functionalized with **4** and the CdS nanoparticles are modified with complementary **2**.

parallel assembly of the layered nanoparticle system on a Au/quartz piezoelectric crystal indicated that the surface coverage of the base dithiol monolayer was 8×10^{-10} mole cm^{-2} and the surface coverage of the gold nanoparticles and the CdS nanoparticles corresponded to 7.0×10^{10} and 2.6×10^{12} particles cm^{-2}, respectively.

Figure 5a, curve 1, shows the absorption spectrum of the primary layer of gold nanoparticles on the gold surface. The characteristic plasmon absorbance is clearly visible at $\lambda=$ 520 nm. From the values of the absorbance and the extinction

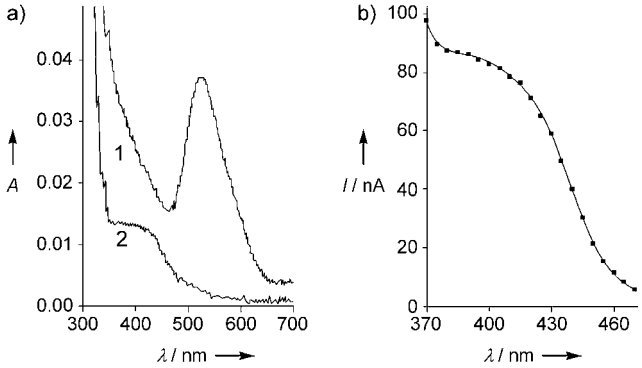

Figure 5. a) Absorbance spectra on a gold-coated glass support of 1) the gold nanoparticle layer and 2) the gold nanoparticle/CdS nanoparticle assembly shown in Figure 4. b) Photocurrent action spectrum corresponding to the gold nanoparticle/CdS nanoparticle assembly. Data recorded in THF solutions containing triethylamine (2×10^{-2} M) and tetra-*n*-butylammonium hexafluorophosphate (0.1 M).

coefficient of 12-nm gold nanoparticles ($\varepsilon=3\times10^{8}$ M^{-1} cm^{-1}),[20] the surface coverage of the gold nanoparticles was estimated to be 6.9×10^{10} particles cm^{-2}, in excellent agreement with the QCM measurements. Figure 5a, curve 2, shows the corrected absorption spectrum of the system after linking the **2**-functionalized CdS nanoparticles to the surface, with the background absorbance of the primary gold nanoparticles subtracted from the spectrum of the composite. The absorbance spectrum of the CdS nanoparticles is clearly identified and exhibits a characteristic shoulder at $\lambda=420$ nm.

Photocurrents from the electrode functionalized with the gold nanoparticle/CdS nanoparticle array were then measured. Figure 5b shows the photocurrent action spectrum of the system. The results are compared to the related hydrogen-bonded CdS nanoparticle assembly that lacks the gold nanoparticles (Figure 1b). The depicted photocurrent action spectra were normalized to exhibit identical surface coverage of the CdS nanoparticles. The photocurrent observed in the gold nanoparticle/CdS nanoparticle composite system is approximately 2.6-fold enhanced relative to the system that lacks the gold nanoparticles. The enhanced photocurrent in the gold nanoparticle/CdS nanoparticle composite system is attributed to the charge separation of the electron–hole pair that is generated upon the photochemical excitation of the CdS nanoparticles; that is, the transfer of the conduction-band electrons to the gold nanoparticles spatially separates the electron–hole pair, thus leading to the retardation of the electron–hole recombination. This delay facilitates the effective scavenging of the valence-band holes by the electron donor as well as the transfer of the electrons trapped by the gold nanoparticles to the electrode, processes that lead to the enhanced generation of photocurrents. There is a substantial difference between the hydrogen-bonded bulk gold surface/CdS nanoparticle configurations (Figure 1a and b) and the hydrogen-bonded gold nanoparticle/CdS nanoparticle array (Figure 4) in facilitating charge separation. A comparison of the surface coverage of molecular components on the functionalized gold nanoparticles or the CdS nanoparticles with the surface coverage by **2**, **4**, or propanedithiol on the bulk gold surfaces indicates that the surface coverage of the bulk gold support is 50- to 100-fold higher than the loadings of the particles. This result implies that the CdS nanoparticles which are linked to the electrode exist in a rigid configuration, whereas structural flexibility exists within the gold nanoparticle/CdS nanoparticle array. This flexibility facilitates the quenching of the conduction-band electrons and enhances charge separation. Furthermore, note that the schematic configuration depicted in Figure 4 is a simplified configuration. The CdS nanoparticles as well as the gold nanoparticles exhibit irregular surface roughness. As a result, the nanoparticles may exist at a substantially closer distance than that dictated by the hydrogen-bonded complex which would facilitate the interparticle charge transport. The special separation of the electron and hole in two different particles then retards the recombination reactions and enhances the photocurrent.

The addition of water to the composite gold nanoparticle/CdS nanoparticle system resulted in the dissociation of the CdS nanoparticles, as observed from microgravimetric QCM measurements, absorption spectra, and photocurrent measurements (see Figure 6). These results imply that the CdS nanoparticles are linked to the gold nanoparticles by complementary hydrogen bonds that are dissociated by water, whereas the gold nanoparticles themselves are tightly bound to the gold support by the dithiol bridging monolayer.

In conclusion, the present study has employed complementary hydrogen bonds to fabricate metal and semiconductor nanoparticle arrays on surfaces and has demonstrated the functional use of the resulting nanostructures for the generation of photocurrents. Although the results may have a limited impact for energy conversion owing to the low photocurrent values, the study highlights fundamental effects

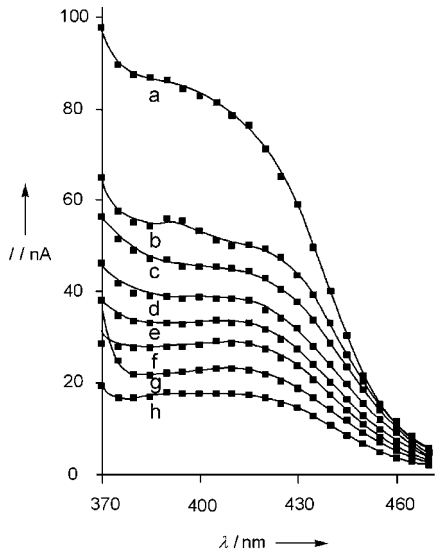

Figure 6. Effect of added water on the photocurrent spectra generated by the gold nanoparticle/CdS nanoparticle assembly shown in Figure 4. Data were recorded in THF solutions containing triethylamine (2×10^{-2} M) and tetra-*n*-butylammonium hexafluorophosphate (0.1 M). Photocurrent spectra were recorded a) before and (b–f) after the addition of 10% water to the solution in THF: b) 4 min, c) 8 min, d) 12 min, e) 16 min, f) 20 min, g) 24 min, and h) 28 min.

of hydrogen-bonded complexes on charge transport at semiconductor nanoparticle/electrode interfaces. The fact that the presented systems are in a monolayer/bilayer nanoparticle configuration suggests, however, that by tailoring hydrogen-bonded composites of higher complexity the resulting photocurrents could be further enhanced.

Experimental Section

Photocurrent experiments were performed using a homebuilt instrument described previously.[7] All spectra were recorded under argon on solutions in THF (0.1M) that contained triethylamine (Et_3N; 2×10^{-2} M) as a sacrificial electron donor and tetra-*n*-butylammonium hexafluorophosphate (0.1M) as electrolyte. The electrodes used were piezoelectric Au/quartz crystals, which allowed us to determine the surface coverage as well as record the photocurrent. The photocurrent spectra were normalized by using the surface coverage of CdS nanoparticles on the piezoelectric crystals.

Absorbance spectra and quantum efficiencies were measured using glass slides coated with a 3-nm layer of chromium and a 50-nm layer of gold (Analytical-μ Systems, Germany). The absorbance spectra were obtained after subtraction of the background absorbance of the gold coating. The quantum efficiency was calculated by determining the light intensity absorbed by the CdS nanoparticle systems and the photocurrent intensities generated by the respective electrodes. The intensity of the light absorbed by the CdS nanoparticle layered system was determined by monitoring the intensity of the light transmitted through the gold-coated glass and the light reflected from the coated surface, and then subtracting the respective values for the transmitted/reflected light for the gold surface modified with CdS nanoparticles. To determine the intensity of absorbed light in the gold nanoparticle/CdS nanoparticle system, the intensity of the transmitted/reflected light in the gold nanoparticle/CdS nanoparticle system was substracted from the intensities of the transmitted/reflected light from the gold surface modified with gold nanoparticles.

Preparation of the CdS nanoparticle assemblies: (The characterization of compounds **1** and **3** is detailed in the Supporting Information.) The acetyl protecting groups in compounds **1** and **3** were removed by hydrolysis under basic conditions in THF by the addition of approximately 10 mg of NH_4OH. CdS nanoparticles, which were prepared according to the reported methods,[15] were capped by mixing solutions of CdS nanoparticles (4 mL) with a solution of **1** or **3** (5×10^{-3} M) in THF (2 mL). The mixture was stirred overnight, then pyridine (0.5 mL) was added, and the resulting particles were collected by centrifugation, washed with THF (×3), and dissolved in THF (2 mL). This solution of nanoparticles was then used to assemble the functionalized electrodes.

The electrode configurations shown in Figure 1a and b were prepared by the following procedure: Au/quartz-crystal electrodes and gold-plated glass electrodes were cleaned in boiling ethanol prior to modification. The electrodes were then modified with either **2** or **4** (5×10^{-3} M overnight in THF) and then immersed for 30 min in the solution of the CdS nanoparticles in THF that were capped with the complementary compound. After each modification step, the electrodes were washed with THF (×3).

For the configuration presented in Figure 4, the electrodes were modified with a propanedithiol monolayer (10^{-2} M, overnight in methanol) and then immersed overnight in an aqueous solution of citrate-stabilized gold nanoparticles. The electrodes were then modified by the procedure described above for the configuration of Figure 1b.

FT-IR spectra were obtained using a Bruker Equinox 55 instrument. The measurements were made directly on gold-coated glass slides in the dry phase under argon, and 1000 scans were averaged for each curve.

The estimation of the number of hydrogen bonds between the CdS nanoparticles and the complementary base monolayer associated with the gold support was based on some rough geometrical approximations. By knowing the average particle diameter, the footprint area of the particles with the monolayer was calculated. By knowing the total loading of the CdS nanoparticles with **2** or **4** (the surface coverage of the gold surface is substantially higher than the coverage of the particles), we were able to estimate the number of hydrogen bonds between the nanoparticles and the surface by also assuming that all the units associated with the footprint area form the hydrogen bonds with the surface.

Received: December 24, 2004
Revised: March 6, 2005
Published online: May 24, 2005

Keywords: gold · hydrogen bonds · nanostructures · photoelectrochemistry · semiconductors

[1] a) A. N. Shipway, E. Katz, I. Willner, *ChemPhysChem* **2000**, *1*, 18–52; b) A. N. Shipway, I. Willner, *Chem. Commun.* **2001**, 2035–2045; c) E. Katz, I. Willner, *Angew. Chem.* **2004**, *116*, 6166–6235; *Angew. Chem. Int. Ed.* **2004**, *43*, 6042–6108.

[2] a) C. Nasr, S. Hotchandani, W. Y. Kim, R. S. Schmehl, P. V. Kamat, *J. Phys. Chem. B* **1997**, *101*, 7480–7487; b) V. Pardo-Yissar, E. Katz, J. Wasserman, I. Willner, *J. Am. Chem. Soc.* **2003**, *125*, 622–623; c) D. Dong, D. Zheng, F.-Q. Wang, X.-Q. Yang, N. Wang, Y.-G. Li, L.-H. Guo, J. Cheng, *Anal. Chem.* **2004**, *76*, 499–501.

[3] a) N.-G. Park, M. G. Kang, K. M. Kim, K. S. Ryu, S. H. Chang, D.-K. Kim, J. van de Lagemaat, K. D. Benkstein, A. J. Frank, *Langmuir* **2004**, *20*, 4246–4253; b) A. Zaban, S. G. Chen, S. Chappel, B. A. Gregg, *Chem. Commun.* **2000**, 2231–2232.

[4] E. Granot, F. Patolsky, I. Willner, *J. Phys. Chem. B* **2004**, *108*, 5875–5881.

[5] a) N. A. Kotov, I. Dekany, J. H. Fendler, *J. Phys. Chem.* **1995**, *99*, 13065 – 13069; b) K. Ariga, Y. Lvov, M. Onda, I. Ichinose, T. Kunitake, *Chem. Lett.* **1997**, 125 – 126; c) Z. Tang, Y. Wang, N. A. Kotov, *Langmuir* **2002**, *18*, 7035 – 7040.
[6] a) V. L. Colvin, A. N. Goldstein, A. P. Alivisatos, *J. Am. Chem. Soc.* **1992**, *114*, 5221 – 5230; b) S. Westenhoff, N. A. Kotov, *J. Am. Chem. Soc.* **2002**, *124*, 2448 – 2449.
[7] L. Sheeney-Haj-Ichia, J. Wasserman, I. Willner, *Adv. Mater.* **2002**, *14*, 1323 – 1326.
[8] L. Sheeney-Haj-Ichia, I. Willner, *J. Phys. Chem. B* **2002**, *106*, 13094 – 13097.
[9] a) L. Sheeney-Haj-Ichia, S. Pogorelova, Y. Gofer, I. Willner, *Adv. Funct. Mater.* **2004**, *14*, 416 – 424; b) L. Sheeney-Haj-Ichia, B. Basnar, I. Willner, *Angew. Chem.* **2005**, *117*, 80 – 85; *Angew. Chem. Int.* Ed. **2005**, *44*, 78 – 83.
[10] a) D. Coman, I. M. Russu, *J. Am. Chem. Soc.* **2003**, *125*, 6626 – 6627; b) M. Peters, I. Rozas, I. Alkorta, J. Elguero, *J. Phys. Chem. B* **2003**, *107*, 323 – 330; c) H.-C. Lin, H.-Y. Sheu, C.-L. Chang, C. Tsai, *J. Mater. Chem.* **2001**, *11*, 2958 – 2965.
[11] S. Mandal, A. Gale, N. Lala, R. Gonnade, V. Gavnir, M. Sastry, *Langmuir* **2001**, *17*, 6262 – 6268.
[12] a) L. Han, J. Luo, N. N. Kariuki, M. M. Maye, V. W. Jones, C. J. Zhong, *Chem. Mater.* **2003**, *15*, 29 – 37; b) A. K. Boal, V. M. Rotello, *Langmuir* **2000**, *16*, 9527 – 9532.
[13] a) A. K. Boal, V. M. Rotello, *J. Am. Chem. Soc.* **2002**, *124*, 5019 – 5024; b) A. Labande, J. Ruiz, D. Astruc, *J. Am. Chem. Soc.* **2002**, *124*, 1782 – 1789; c) U. Drechsler, B. Erdogan, V. Rotello, *Chem. Eur. J.* **2004**, *10*, 5570 – 5579.
[14] E. Hao, T. Lian, *Chem. Mater.* **2000**, *12*, 3392 – 3396.
[15] M. Miyake, H. Matsumoto, M. Nishizawa, T. Sakata, H. Mori, S. Kuwabata, H. Yoneyama, *Langmuir* **1997**, *13*, 742 – 746.
[16] W. W. Yu, L. Qu, W. Guo, X. Peng, *Chem. Mater.* **2003**, *15*, 2854 – 2860.
[17] W.-S. Yang, S.-G. Chen, X.-D. Chai, Y.-W Cao, R. Lu, W.-P. Chai, Y.-J. Jiang, T.-J. Li, J.-M. Lehn, *Synth. Met.* **1995**, 71, 2107 – 2108.
[18] Z. Sideratou, D. Tsiourvas, C. M. Paleos, E. Peppas, J. Anastassopoulou, T. Theophanides, *J. Mol. Struct.* **1999**, *484*, 91 – 101.
[19] K. C. Grabar, R. G. Freeman, M. B. Hommer, M. J. Natan, *Anal. Chem.* **1995**, *67*, 735 – 743.
[20] S. Link, M. El-Sayed, *J. Phys. Chem. B* **1999**, *103*, 8410 – 8426.

